



**HAL**  
open science

## Concentration-dependent characteristics of a complex coacervate

Hongwei Li, Lionel Porcar, Ahmed Bentaleb, Christophe Schatz, Jean-Paul Chapel

► **To cite this version:**

Hongwei Li, Lionel Porcar, Ahmed Bentaleb, Christophe Schatz, Jean-Paul Chapel. Concentration-dependent characteristics of a complex coacervate. 2022. hal-03839081

**HAL Id: hal-03839081**

**<https://hal.science/hal-03839081>**

Preprint submitted on 4 Nov 2022

**HAL** is a multi-disciplinary open access archive for the deposit and dissemination of scientific research documents, whether they are published or not. The documents may come from teaching and research institutions in France or abroad, or from public or private research centers.

L'archive ouverte pluridisciplinaire **HAL**, est destinée au dépôt et à la diffusion de documents scientifiques de niveau recherche, publiés ou non, émanant des établissements d'enseignement et de recherche français ou étrangers, des laboratoires publics ou privés.



Distributed under a Creative Commons Attribution - NonCommercial - NoDerivatives 4.0 International License

# Concentration-dependent characteristics of a complex coacervate

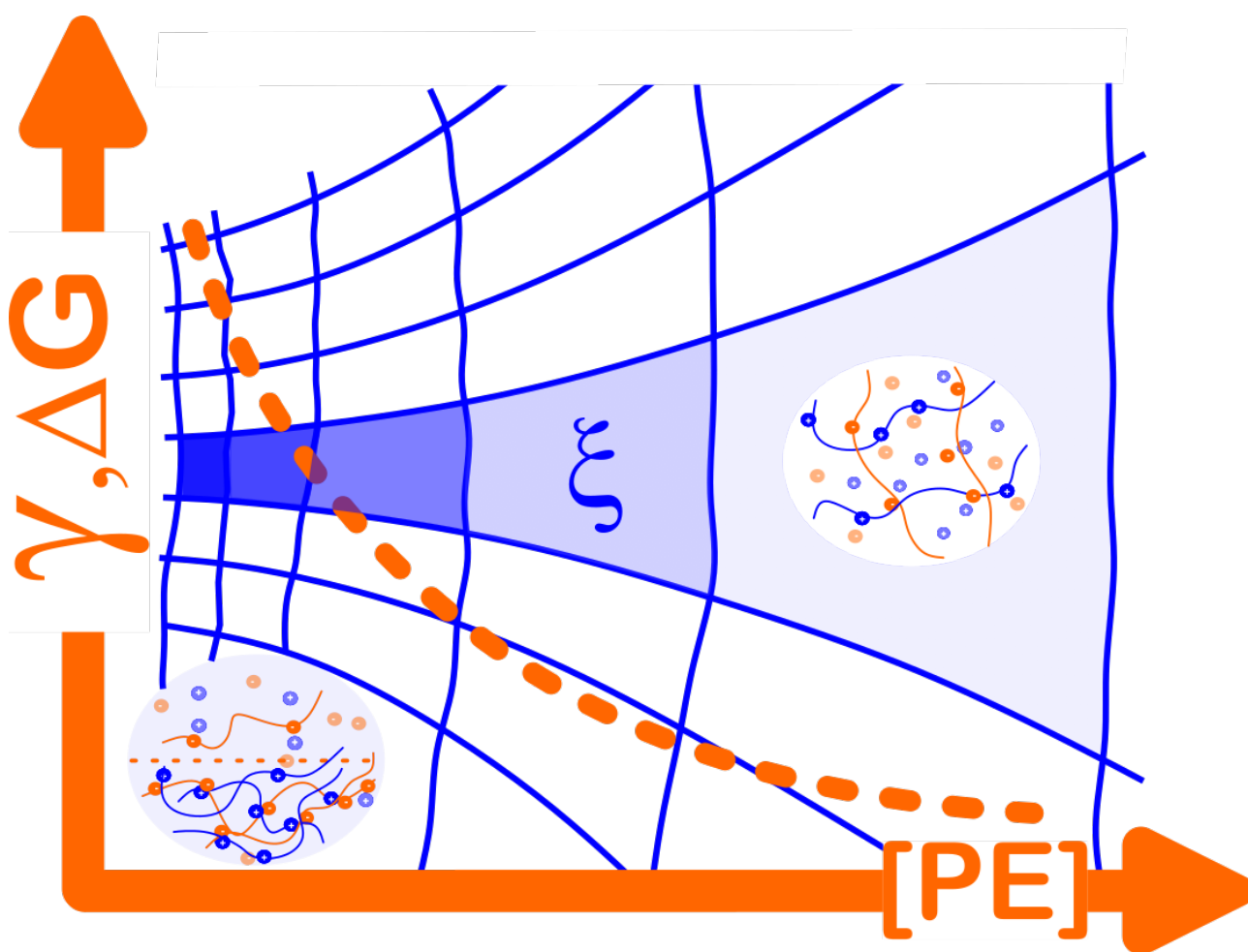
Hongwei Li<sup>1,2</sup>, Lionel Porcar<sup>3</sup>, Amhed Bentaleb<sup>1</sup>, Christophe Schatz<sup>2</sup> and Jean-Paul Chapel<sup>1</sup>

<sup>1</sup> Centre de Recherche Paul Pascal, Univ. Bordeaux, CNRS, CRPP, UMR 5031, F-33600 Pessac, France

<sup>2</sup> Laboratoire de Chimie des Polymères Organiques, Univ. Bordeaux, CNRS, Bordeaux INP, LCPO, UMR 5629, F-33600 Pessac, France

<sup>3</sup> Institut Laue-Langevin, 71 Avenue des Martyrs, 38042 Grenoble Cedex 9, France

\* Correspondence: schatz@enscbp.fr (C.S.); jean-paul.chapel@crpp.cnrs.fr (J.-P.C.)



**Abstract:** In this work, we have comprehensively and systematically investigated the influence of the initial concentration of oppositely charged polyelectrolyte solutions on the interaction strength, interfacial tension and local structure of the coacervate phase generated at charge stoichiometry in a PDADMAC/PANa model system. We have shown for the first time that the concentration has a direct and significant impact on the complexation strength between the two polyelectrolytes, leading to lighter coacervates with constant mass yield and increasing network mesh and decreasing liquid-liquid interfacial tensions until a critical concentration where oppositely charged chains no longer interact, generating the so-called self-suppressed coacervate single phase (SSCV). An effect that is due to the free counterions present in the solution, whose concentration increases with that of the PE polyelectrolytes and gradually screens the electrostatic complexation. These characteristics will certainly have an impact on the capacity of these coacervates, objects of great scientific and technical interest today, to be efficiently stabilized, to encapsulate active principles and to serve as bioreactors.

Keywords: polyelectrolyte complexes; complex coacervate; electrostatic interaction; complexation strength; interfacial tension; thermodynamic; local structures; morphologies

The complexation of oppositely charged polyelectrolytes (PEs) in aqueous solutions is a widespread associative process in natural and artificial systems, which proceeds through primarily cooperative electrostatic interactions. Complementary interactions like short-range hydrogen-bonding or long-range hydrophobic effect can also participate in the complexation process. These PE complexes or PECs have endless applications in different technological fields ranging from water treatment<sup>1</sup>, paper making<sup>2</sup> and food industry<sup>3</sup> to pharmaceuticals<sup>4</sup>, cosmetics<sup>5</sup>, tissue engineering<sup>6</sup> and biomedicine<sup>7</sup>. The formation of PECs involves two distinct steps: the generation of primary PECs by ion pairing, followed by their aggregation/reorganization into larger structures.<sup>8-9</sup> When the oppositely charged PE mixture is not at charge stoichiometry, complexation typically results in colloidal polyelectrolyte complexes where the excess PE forms an electrosterically stabilizing shell around the neutral complexed cores<sup>10</sup> with a solvation, charge, hydrophobicity that vary with the molar charge ratio  $Z\{[-]/[+]\}$ .<sup>9, 11-14</sup> At charge stoichiometry, when the amount of anionic and cationic charges are equal, two very different situations can occur depending on the strength of the interaction. When the charged chains are in strong interaction (binding constant  $k_b > 10^6 \text{ M}^{-1}$ ), the system undergoes a liquid-solid transition generating aggregates that eventually sediment with time as in the case of the well-known PDADMAC/PSSNa system.<sup>9, 14-16</sup> When the interaction is weaker, the system undergoes a liquid-liquid phase transition generating highly hydrated and dense chemically enriched microdroplets in equilibrium with the surrounding macromolecule-depleted continuous phase as in the PDADMAC/PANa system ( $k_b \sim 10^3 - 10^4 \text{ M}^{-1}$ ).<sup>11-14</sup> These complex coacervate phases have emerged in recent years as promising compartments for the construction of rudimentary forms of artificial cells.<sup>17-18</sup> Due to their differential chemical composition and physical properties compared to the continuous phase, these crowded droplets spontaneously and selectively accumulate various solutes,<sup>17-18</sup> including molecular dyes<sup>19</sup>, proteins or polynucleotides<sup>20</sup>. This effect due to the peculiar physicochemical environment found in the coacervate phase provides a simple way to localize and concentrate functional species, although the exact mechanism is not yet known, partly because the local structure of this phase and the parameters that influence it are not systematically studied in the literature. In particular, in most studies of complex coacervation, the polyelectrolyte concentration is held constant and the ionic strength and/or molecular weight of the chains are often used as adjustable

parameters to study the phase diagram. The impact of the overall polyelectrolyte concentration is rarely studied in a systematic way in the literature, especially for high values.<sup>21</sup>

Herein, we comprehensively and systematically investigated the influence of polyelectrolyte concentration on the final properties of a model PDADMAC/PANa complex coacervate phase generated at charge stoichiometry. We will examine the impact of formulation concentration on the interaction strength, interfacial tension, and local structure of this polymer-rich phase in equilibrium with its supernatant using complementary techniques such as thermo-gravimetric analysis (TGA), dynamic light scattering (DLS), small angle neutron scattering (SANS), and interfacial tension measurements.

We have generated mixtures at charge stoichiometry made at increasing polyelectrolyte (PE) concentration. After preparation, each coacervate phase was allowed to stand for 2 weeks to allow the system to equilibrate. A clear macroscopic phase separation between a light supernatant and a denser coacervate phase (CCV) was generated for all concentrations up to 0.85M, where coacervation was unexpectedly suppressed giving rise to a single phase as shown in **Figure 1(a)**, the so-called self-suppressed coacervate phase (SSCV).<sup>21-22</sup> To better characterize the system macroscopically, we performed density and thermogravimetric analyses. Strikingly, the density of the supernatant increases linearly with the PE concentration while that of the coacervate decreases symmetrically (**Figure 1(b,c)**). When the PE concentration increases, the generated coacervate phase becomes lighter and the supernatant denser until a critical concentration where the two curves cross and coacervation is suppressed, resulting in a single phase (SSCV) in agreement with visual observations.

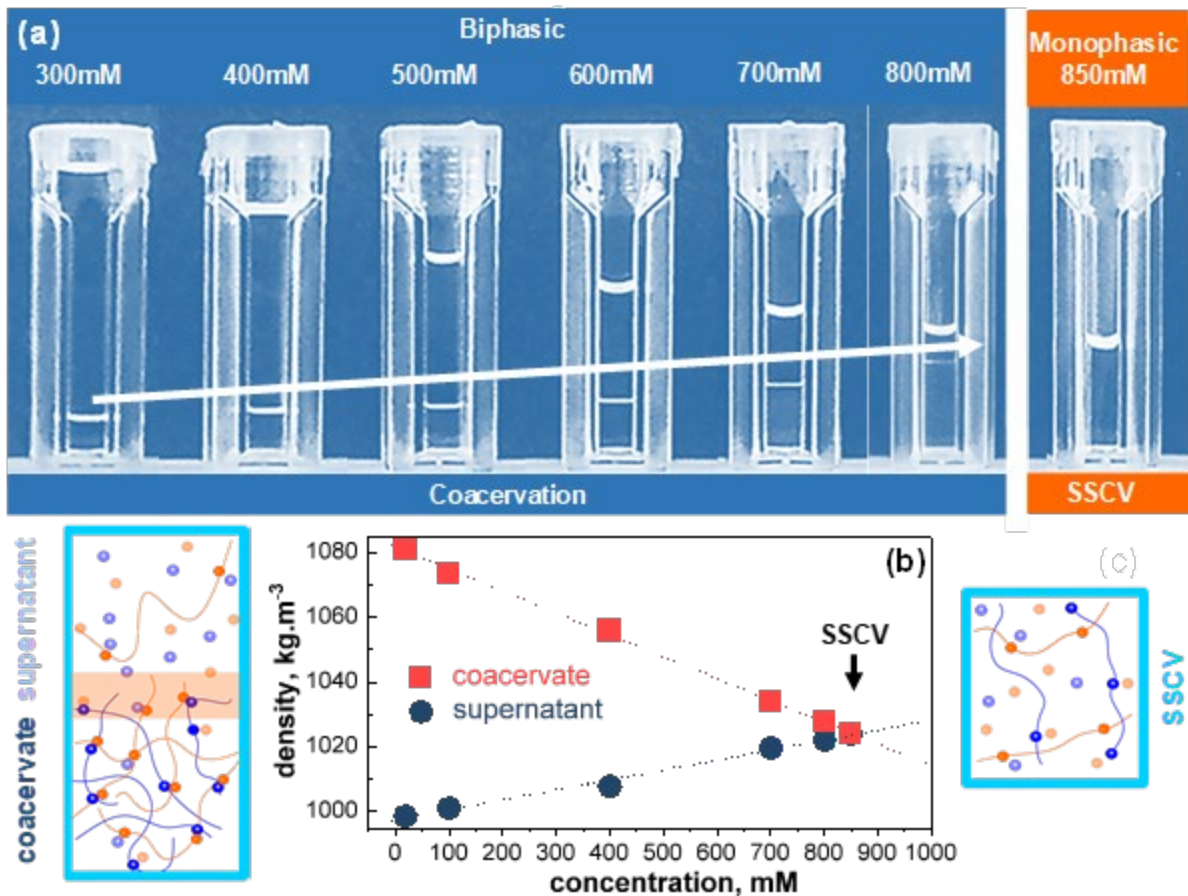


**Figure 1.** (a) Photographs of the mixtures generated at charge stoichiometry at increasing PE concentration. Above 0.85M coacervation is suppressed giving way to a single phase (SSCV). (b) Variation of supernatant and coacervate density  $\rho$  with PE concentration. The dotted lines are a linear fit of the data.

TGA measurements were then performed to accurately estimate the overall PE content, including counterions. As anticipated, the PE mass fraction in the coacervate is much higher than in the supernatant at low concentrations (**Figure S2**) and decreases with increasing concentration, while that of the supernatant increases. The coacervate and supernatant phases become linearly lighter and denser, respectively, with increasing PE concentration. Furthermore, by measuring the height ratio between the coacervate phase and the total solution in **Figure 1**, we can calculate the coacervate volume fraction and estimate its volume yield. The volume fraction increases with the PE concentration resulting in an apparent increase in production yield (**Figure S2(c)**). We can finally calculate the polymer mass yield defined as  $m_{CCV}/m_{total}$ . Remarkably, the polymer mass yield appears constant in each phase, with no polymer gain or loss. As we will see later, only the internal structure of the CCV phase changes.

Recently we have shown that surface tension measurements are a very sensitive tool to study the structure and formation mechanism of polyelectrolyte complexes (PECS).<sup>14</sup> With this in mind, we have measured the surface tension of the supernatant ( $\gamma_s$ ) and the interfacial tension ( $\gamma_{cc}$ ) between the coacervate and the supernatant as a function of PE concentration. As anticipated from density data,  $\gamma_s$  decreases with PE concentration, consistent with increasingly dense supernatants and stronger adsorption of PECs at the air-water interface. At ~850 mM, where coacervation is suppressed,  $\gamma_s$  is lowest (**Figure S4**). An effect qualitatively similar to that of where the surface tension decreases with concentration due to the screening effect of free counterions.<sup>14</sup> Furthermore, to calculate the interfacial tension  $\gamma_{cc}$ , the capillary length  $l_c (= \sqrt{\frac{\gamma_{cc}}{\Delta\rho * g}})$  was measured by analyzing the static interfacial profile near the vertical wall of a cell with a shape given by the generalized Young-Laplace equation connecting capillary pressure with curvature and surface tension for a flat wall (**SI Material & method**). It can be seen in **Figure S4** that the four extracted static profiles are different suggesting that  $\gamma_{cc}$  indeed varies with the concentration.  $\gamma_{cc}$  clearly decreases with the concentration as shown **Figure 2** until a critical value of about 850mM where coacervation is suppressed and  $\gamma_{cc} \equiv 0$ . Photographs, TGA, density and surface tension measurements all suggest the presence of a single phase as the concentration increases, where the two PE no longer interact.

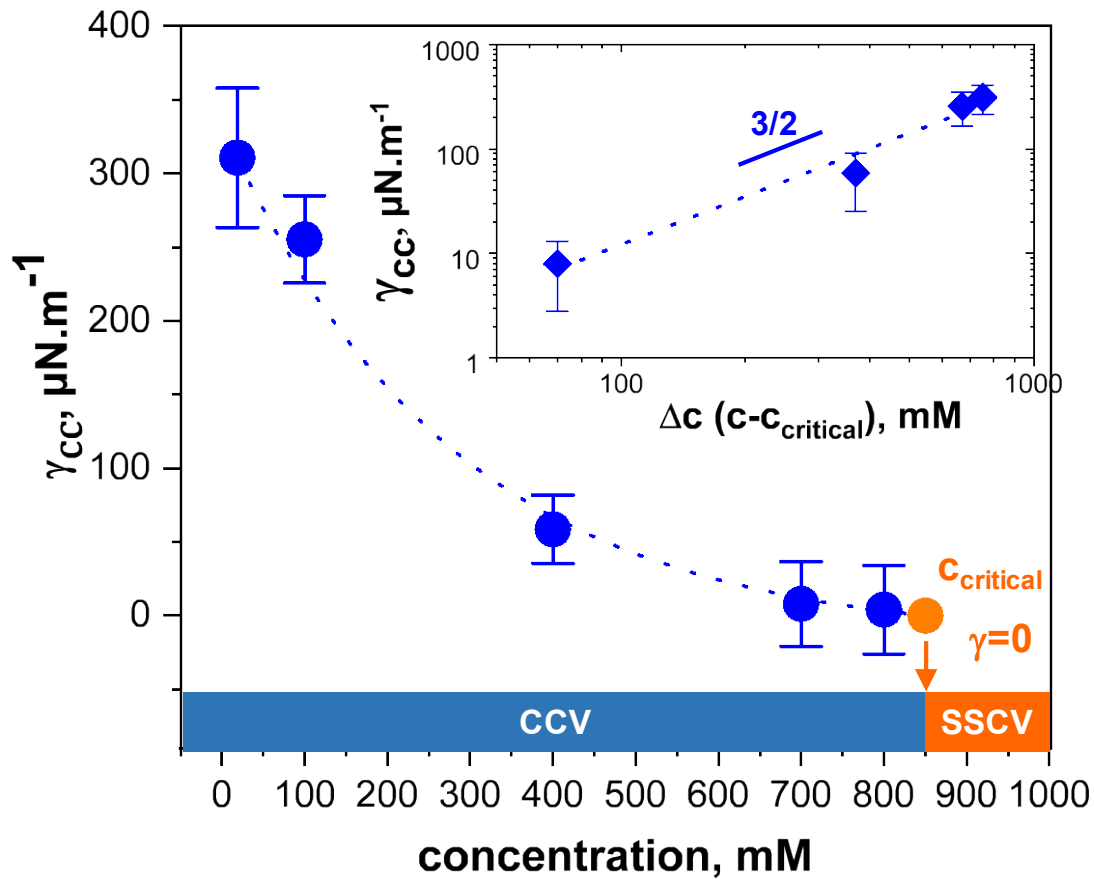


**Figure 2.** Liquid-liquid interfacial tension  $\gamma_{cc}$  between the supernatant and the coacervate as a function of the PE concentration. At the critical concentration, coacervation is suppressed and  $\gamma_{cc} = 0$ . Insert : Log-Log representation of  $\gamma_{cc}$  as a function of  $\Delta c$ . The dotted line is a linear fit.

Spruijt *et al.* were the first to measure the interfacial tension of a symmetric complex coacervate using surface colloidal probe AFM measurements.<sup>23</sup> They showed that at a given (and low) PE concentration,  $\gamma_{cc}$  decreases with increasing salt concentration  $\varphi_s$  as  $\gamma \sim |\varphi_{s-critical} - \varphi_s|^{3/2}$  near the critical concentration  $\varphi_{s-c}$  where coacervation disappears. This particular salt dependence was confirmed experimentally and theoretically by Priftis *et al.*<sup>24</sup>, Ali *et al.*<sup>25</sup> and Qin *et al.* who have rationalized this scaling law by combining the Voorn–Overbeek theory with the Cahn–Hilliard mathematical theory (Figure S5).<sup>26</sup> If we plot our data as a function of  $\Delta c = c - c_{SSCV}$  with  $c$  the PE concentration and  $c_{SSCV}$  the critical concentration at which coacervation is suppressed (insert Figure 2), we find a linear variation (Log-Log) with a slope of 3/2 strikingly similar to Figure S5. The interfacial tension between the coacervate and supernatant then varies similarly with increasing salt or PE concentration, suggesting that the ionic strength generated by the free counterions has a similar effect on the interfacial tension as added salt. In a recent work, we showed that the ionic strength generated by the free counterions was responsible for the decrease in surface tension



with PE concentration.<sup>14</sup> It is therefore conceivable that such an increase in ionic strength is also responsible for the suppression of coacervation. The concentration of free counterions is known to increase linearly as  $C_c = C_{PE} f_{eff}$ , with  $f_{eff}$  the effective charged fraction of polymer units (SI). At  $C_{SSCV}$ , the ionic strength (I) of the mixture can then be estimated from the total concentration of free counterions :  $I = \frac{1}{2} \sum C_i z_i^2 = \frac{1}{2} * (C_{PDAD} f_{eff} + C_{PANa} f_{eff}) = 0.37M$ . A value not far from the desalting transition concentration measured around 0.3M in our system.<sup>27</sup> At this point, the ionic strength of the free counterions can therefore rationalize our observations on the variation of the interfacial energy up to a critical concentration at which coacervation is suppressed.<sup>21</sup>

To further investigate the local structure of these phases, static small angle neutron scattering (SANS) and dynamic light scattering (DLS) measurements were performed. For PE solutions in the semi-dilute regime, it is known that overlap between chains leads to the formation of a transient network with characteristic correlation length  $\xi$ . Sections of a chain smaller than  $\xi$  will be fully stretched, while for distances greater than  $\xi$ , electrostatic interactions are screened out and, therefore, the chains can be pictured as ideal chains of  $\xi$  length segments.<sup>28</sup> **Figure 3(a)** shows DLS data where two distinct relaxation modes are observed for concentrations below 900 mM. The fast mode corresponds to the relaxation of  $\xi$ -sized polymer segments forming so-called blob subunits while the slower mode is associated to large transient aggregates heterogeneities in the coacervate phase. When the coacervate volume fraction increases, larger aggregates are expected to form through potential dipole-dipole pairings.<sup>29</sup> Interestingly, in the SSCV phase where the PEs no longer interact, the slow relaxation disappears. The relaxation associated with blob diffusion is faster for lower PE concentrations (dense coacervate) (**Figure S7(b)**) suggesting that blobs are smaller at low concentrations. This is exactly the opposite of concentrated solutions of neutral polymers in a good solvent, where the blob size decreases with polymer concentration.<sup>30</sup>

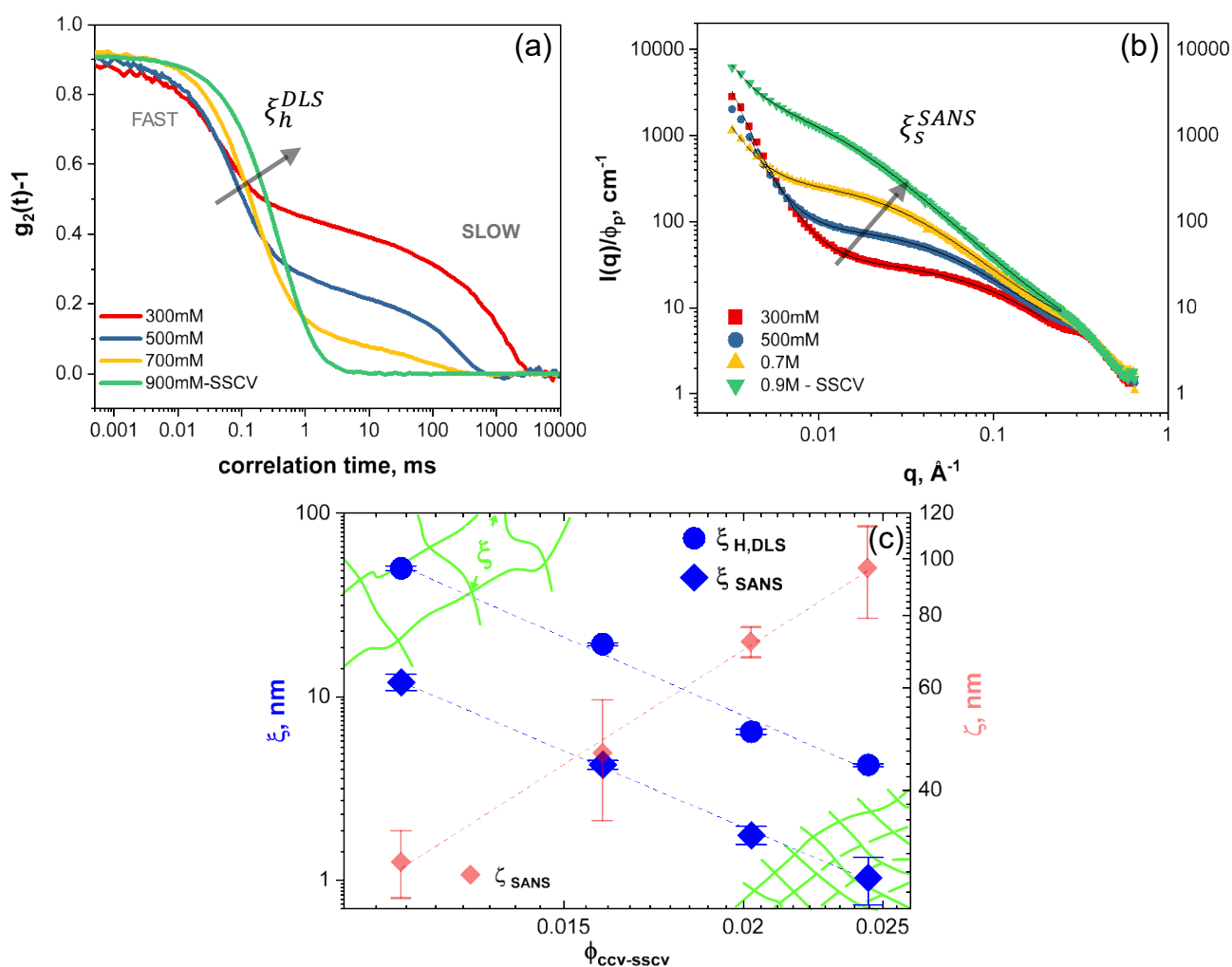


**Figure 3. (a)** DLS - Intensity correlation functions taken at a scattering angle of  $90^\circ$ . **(b)** SANS signature. The scattered intensity has been renormalized by  $\varphi_{phase}$ . Black lines are an Ornstein-Zernike (OZ)-Debye-Bueche (DB) fit to the data (low-mid  $q$ ). **(c)** Correlation lengths  $\xi$  and inhomogeneity sizes  $\zeta$  as a function of  $\varphi_{phase}$ .

To accurately determine the correlation length associated with the fast mode we measured the correlation functions (**Figure S8**) and distribution of decay times (**Figure S9**) over a wide range angles from  $30^\circ$  to  $150^\circ$ . The trend is similar with decay times going to lower values and the appearance of a slow mode as the PE concentration decreases. **Figure 3(c)** shows in a Log-Log representation a linear decrease of the hydrodynamic correlation length  $\xi_H$  (SI for details) with the phase volume fraction  $\varphi_{phase}$ . As the concentration increases, the coacervates become lighter with slower relaxing networks in full agreement with lower collective diffusion coefficients  $D$  or longer  $\xi_H$ . Furthermore, the SANS signature varies significantly within

each phase (**Figure 3(b)**), suggesting that the local structure also varies with concentration. In addition, the incoherent scattering decreases linearly with increasing PE concentration, in perfect agreement with the TGA/density measurements (**Figure S11(b)**). In the mid and high  $q$  region, the PE chains overlap in the complex coacervate phase, like a semi-dilute polymer solution at equilibrium. It should then follow the Ornstein-Zernike (OZ) structure factor accounting for the concentration fluctuations at high  $q$ .<sup>31</sup> Excessive low- $q$  scattering, always present in PE solutions, and attributed to local inhomogeneities many times their  $R_g$ <sup>32</sup>, can also be well captured by a Debye-Bueche(DB) structure factor<sup>33</sup> that accounts for scattering by an inhomogeneous solid (**SI for details**). Overall, the OZ-DB structure factor model accounts for the SANS data particularly well. We can see from **Figure 3(c)** that the variation of the dynamic (DLS) and static (SANS) correlation lengths agree well and scale with  $\xi_H \sim (\varphi_{phase})^{-\beta}$  ( $\beta \sim 3.31$  and  $3.4$  for DLS and SANS respectively). Hydrodynamic  $\xi_H$  values are, as expected higher than static values. The size of the transient inhomogeneities  $\zeta$  decreases with increasing concentration in agreement with decreasing dipole-dipole interactions. Furthermore, if we look more closely above  $0.2 \text{ \AA}^{-1}$  (**Figure S11(a)**) we observe a distinct correlation peak for each coacervate phase that decreases in intensity and moves to smaller  $q$  values as  $\varphi_{phase}$  decreases, and eventually disappears into the self-suppressed single phase.

The variation of the local structure and interfacial tension as a function of concentration can then have an impact on some key properties of coacervates. Their very low interfacial tension allows them to effectively encapsulate actives of interest, but also makes them very difficult to stabilize.<sup>34-35</sup> From scaling laws arguments, the interfacial tension at a fluid-fluid interface should scale as  $\gamma \sim k_B T / \delta^2$  where  $\delta$  is the interfacial thickness length scale<sup>36-37</sup> which can then span tens of nm.<sup>38-39</sup> A 4-fold change is foreseen in the PDADMAC/PSSNa system. The type and size of stabilizing agents, the actives to be encapsulated and their mechanisms of action might then drastically change with the initial PE concentration.

## Conclusion

In this work, we comprehensively and systematically investigated the influence of the initial concentration of oppositely charged PE on the interaction strength,

interfacial tension and local structure of a PDADMAC/PANa system at charge stoichiometry. We found that the PE concentration has a direct and significant impact on the coacervate properties. When the PE concentration increases, the complexation strength decreases generating lighter coacervates with increasing network mesh sizes and decreasing liquid-liquid interfacial tensions until a critical concentration where oppositely charged chains no longer interact, generating the so-called self-suppressed coacervate single phase (SSCV). This effect is due to the free counterions present in the solution, whose concentration increases with that of the polyelectrolytes and gradually screens the electrostatic interaction until a critical concentration where the complexation is suppressed. Coacervates have gained a renewed interest recently generated by the discovery of the presence of membrane-less organelles in living cells, identified as immiscible liquid phases forming a coacervate-like phase.<sup>17, 40</sup> It is therefore very important to be aware of the strong impact of the initial PE concentration, the complexation strength, interfacial tension  $\gamma_{cc}$  and thickness  $\delta$ , network local mesh size  $\xi$ , density when formulating coacervate droplets for (bio) technological applications. Characteristics that will certainly have an impact on their ability to be efficiently stabilized, to encapsulate actives, or to serve as a bioreactor. Preliminary experiments have shown that similar effects occur in segregative liquid-liquid phase separation such as the widely studied and used aqueous two-phase systems (ATPS).<sup>41</sup>

## References

- (1).Wilts, E. M.; Herzberger, J.; Long, T. E., Addressing water scarcity: cationic polyelectrolytes in water treatment and purification. *Polymer International* **2018**, *67* (7), 799-814.
- (2).Schnell, C. N.; Tarrés, Q.; Galván, M. V.; Mocchiutti, P.; Delgado-Aguilar, M.; Zanuttini, M. A.; Mutjé, P., Polyelectrolyte complexes for assisting the application of lignocellulosic micro/nanofibers in papermaking. *Cellulose* **2018**, *25* (10), 6083-6092.
- (3).Schmitt, C.; Turgeon, S. L., Protein/polysaccharide complexes and coacervates in food systems. *Advances in Colloid and Interface Science* **2011**, *167* (1), 63-70.
- (4).Meka, V. S.; Sing, M. K. G.; Pichika, M. R.; Nali, S. R.; Kolapalli, V. R. M.; Kesharwani, P., A comprehensive review on polyelectrolyte complexes. *Drug Discovery Today* **2017**, *22* (11), 1697-1706.
- (5).Llamas, S.; Guzman, E.; Ortega, F.; Baghdadli, N.; Cazeneuve, C.; Rubio, R. G.; Luengo, G. S., Adsorption of polyelectrolytes and polyelectrolytes-surfactant mixtures at surfaces: a

physico-chemical approach to a cosmetic challenge. *Adv Colloid Interface Sci* **2015**, *222*, 461-87.

(6).Shakshi, R.; Pramod Kumar, S.; Rishabha, M., Pharmaceutical and Tissue Engineering Applications of Polyelectrolyte Complexes. *Current Smart Materials* **2018**, *3* (1), 21-31.

(7).Buriuli, M.; Verma, D., Polyelectrolyte Complexes (PECs) for Biomedical Applications. In *Advances in Biomaterials for Biomedical Applications*, Tripathi, A.; Melo, J. S., Eds. Springer Singapore: Singapore, 2017; pp 45-93.

(8).Lebovka, N. I., Aggregation of Charged Colloidal Particles. In *Polyelectrolyte Complexes in the Dispersed and Solid State I: Principles and Theory*, Müller, M., Ed. Springer Berlin Heidelberg: Berlin, Heidelberg, 2014; pp 57-96.

(9).Jemili, N.; Fauquignon, M.; Grau, E.; Fatin-Rouge, N.; Dole, F.; Chapel, J.-P.; Essafi, W.; Schatz, C., Complexation in Aqueous Solution of a Hydrophobic Polyanion (PSSNa) Bearing Different Charge Densities with a Hydrophilic Polycation (PDADMAC). *Polymers* **2022**, *14* (12), 2404.

(10).Dautzenberg, H.; Hartmann, J.; Grunewald, S.; Brand, F., Stoichiometry and structure of polyelectrolyte complex particles in diluted solutions. *Berichte der Bunsengesellschaft für physikalische Chemie* **1996**, *100* (6), 1024-1032.

(11).Liu, X.; Chapel, J. P.; Schatz, C., Structure, thermodynamic and kinetic signatures of a synthetic polyelectrolyte coacervating system. *Adv Colloid Interface Sci* **2017**, *239*, 178-186.

(12).Liu, X.; Haddou, M.; Grillo, I.; Mana, Z.; Chapel, J. P.; Schatz, C., Early stage kinetics of polyelectrolyte complex coacervation monitored through stopped-flow light scattering. *Soft Matter* **2016**, *12* (44), 9030-9038.

(13).Vitorazi, L.; Ould-Moussa, N.; Sekar, S.; Fresnais, J.; Loh, W.; Chapel, J. P.; Berret, J. F., Evidence of a two-step process and pathway dependency in the thermodynamics of poly(diallyldimethylammonium chloride)/poly(sodium acrylate) complexation. *Soft Matter* **2014**, *10* (47), 9496-9505.

(14).Li, H.; Fauquignon, M.; Haddou, M.; Schatz, C.; Chapel, J.-P., Interfacial Behavior of Solid- and Liquid-like Polyelectrolyte Complexes as a Function of Charge Stoichiometry. *Polymers* **2021**, *13* (21), 3848.

(15).Fu, J.; Schlenoff, J. B., Driving Forces for Oppositely Charged Polyion Association in Aqueous Solutions: Enthalpic, Entropic, but Not Electrostatic. *Journal of the American Chemical Society* **2016**, *138* (3), 980-990.

(16).Wang, Q.; Schlenoff, J. B., The Polyelectrolyte Complex/Coacervate Continuum. *Macromolecules* **2014**, *47* (9), 3108-3116.

(17).Koga, S.; Williams, D. S.; Perriman, A. W.; Mann, S., Peptide–nucleotide microdroplets as a step towards a membrane-free protocell model. *Nature Chemistry* **2011**, *3* (9), 720-724.

(18).Buddingh', B. C.; van Hest, J. C. M., Artificial Cells: Synthetic Compartments with Life-like Functionality and Adaptivity. *Accounts of Chemical Research* **2017**, *50* (4), 769-777.

(19).Keating, C. D., Aqueous Phase Separation as a Possible Route to Compartmentalization of Biological Molecules. *Accounts of Chemical Research* **2012**, *45* (12), 2114-2124.

(20).Martin, N.; Tian, L.; Spencer, D.; Coutable-Pennarun, A.; Anderson, J. L. R.; Mann, S., Photoswitchable Phase Separation and Oligonucleotide Trafficking in DNA Coacervate Microdroplets. *Angewandte Chemie International Edition* **2019**, *58* (41), 14594-14598.

- (21).Li, L.; Srivastava, S.; Andreev, M.; Marciel, A. B.; de Pablo, J. J.; Tirrell, M. V., Phase Behavior and Salt Partitioning in Polyelectrolyte Complex Coacervates. *Macromolecules* **2018**, *51* (8), 2988-2995.
- (22).Veis, A.; Bodor, E.; Mussell, S., Molecular weight fractionation and the self-suppression of complex coacervation. *Biopolymers* **1967**, *5* (1), 37-59.
- (23).Spruijt, E.; Sprakel, J.; Cohen Stuart, M. A.; van der Gucht, J., Interfacial tension between a complex coacervate phase and its coexisting aqueous phase. *Soft Matter* **2010**, *6* (1), 172-178.
- (24).Priftis, D.; Farina, R.; Tirrell, M., Interfacial Energy of Polypeptide Complex Coacervates Measured via Capillary Adhesion. *Langmuir* **2012**, *28* (23), 8721-8729.
- (25).Ali, S.; Prabhu, V. M., Characterization of the Ultralow Interfacial Tension in Liquid-Liquid Phase Separated Polyelectrolyte Complex Coacervates by the Deformed Drop Retraction Method. *Macromolecules* **2019**, *52* (19), 7495-7502.
- (26).Qin, J.; Priftis, D.; Farina, R.; Perry, S. L.; Leon, L.; Whitmer, J.; Hoffmann, K.; Tirrell, M.; de Pablo, J. J., Interfacial Tension of Polyelectrolyte Complex Coacervate Phases. *ACS Macro Letters* **2014**, *3* (6), 565-568.
- (27).Giermanska, J.; Sekar, S.; Ly, I.; Chapel, J.-P., Influence of the formulation pathway on the growth of polyelectrolyte multilayer films. *Colloids and Surfaces A: Physicochemical and Engineering Aspects* **2016**, *509*, 666-674.
- (28).Mandel, M., Application of dynamic light scattering to polyelectrolytes in solution. In *Dynamic light scattering: the method and some applications*, Brown, W., Ed. Oxford University Press, 1993.: New-York, 1993.
- (29).Muthukumar, M., Ordinary-extraordinary transition in dynamics of solutions of charged macromolecules. *Proceedings of the National Academy of Sciences* **2016**, *113* (45), 12627-12632.
- (30).Jian, T.; Vlassopoulos, D.; Fytas, G.; Pakula, T.; Brown, W., Coupling of concentration fluctuations to viscoelasticity in highly concentrated polymer solutions. *Colloid and Polymer Science* **1996**, *274* (11), 1033-1043.
- (31).Spruijt, E.; Leermakers, F. A. M.; Fokkink, R.; Schweins, R.; van Well, A. A.; Cohen Stuart, M. A.; van der Gucht, J., Structure and Dynamics of Polyelectrolyte Complex Coacervates Studied by Scattering of Neutrons, X-rays, and Light. *Macromolecules* **2013**, *46* (11), 4596-4605.
- (32).Koberstein, J. T.; Picot, C.; Benoit, H., Light and neutron scattering studies of excess low-angle scattering in moderately concentrated polystyrene solutions. *Polymer* **1985**, *26* (5), 673-681.
- (33).Debye, P.; Bueche, A. M., Scattering by an Inhomogeneous Solid. *Journal of Applied Physics* **1949**, *20* (6), 518-525.
- (34).Esquena, J., Water-in-water (W/W) emulsions. *Current Opinion in Colloid & Interface Science* **2016**, *25*, 109-119.
- (35).Douliez, J.-P.; Martin, N.; Beneyton, T.; Eloi, J.-C.; Chapel, J.-P.; Navailles, L.; Baret, J.-C.; Mann, S.; Béven, L., Preparation of Swellable Hydrogel-Containing Colloidosomes from Aqueous Two-Phase Pickering Emulsion Droplets. *Angewandte Chemie International Edition* **2018**, *57* (26), 7780-7784.

(36).de Hoog, E. H. A.; Lekkerkerker, H. N. W., Measurement of the Interfacial Tension of a Phase-Separated Colloid-Polymer Suspension. *The Journal of Physical Chemistry B* **1999**, *103* (25), 5274-5279.

(37).Gennes, P.-G., *Scaling Concepts in Polymer Physics* Cornell Univ. Press: 1979.

(38).Vis, M.; Opdam, J.; van 't Oor, I. S. J.; Soligno, G.; van Roij, R.; Tromp, R. H.; Ern , B. H., Water-in-Water Emulsions Stabilized by Nanoplates. *ACS Macro Letters* **2015**, *4* (9), 965-968.

(39).Scholten, E.; Sagis, L. M. C.; van der Linden, E., Bending Rigidity of Interfaces in Aqueous Phase-Separated Biopolymer Mixtures. *The Journal of Physical Chemistry B* **2004**, *108* (32), 12164-12169.

(40).Yewdall, N. A.; Andr , A. A. M.; Lu, T.; Spruijt, E., Coacervates as models of membraneless organelles. *Current Opinion in Colloid & Interface Science* **2021**, *52*, 101416.

(41).Perro, A.; Coudon, N.; Chapel, J. P.; Martin, N.; B ven, L.; Douliez, J. P., Building microcapsules using water-in-water emulsion droplets as templates. *J Colloid Interface Sci* **2022**, *613*, 681-696.